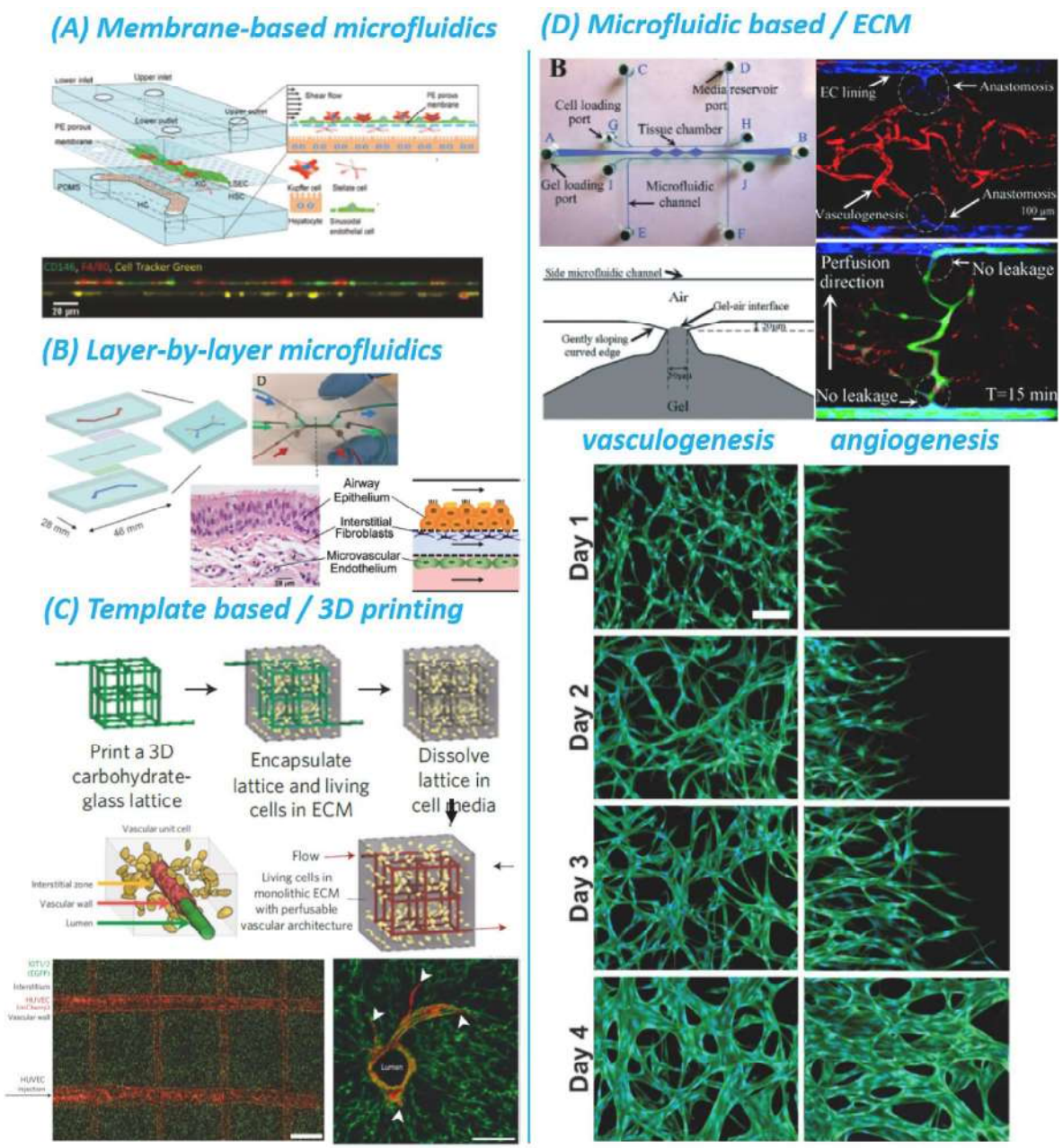

Fig. 7. Schematic representation of methods employed to vascularize 3D OOC models. These techniques can be divided into soft-lithography and 3D patterning approaches. **(A)** Membrane-based soft lithography technique in which a porous membrane is inserted among two microfluidic channels. Reproduced from Ref. (Du et al., 2017). **(B)** Layer-by-layer microfluidics consisting of assembled modular layers. Reproduced from Ref. (Sellgren et al., 2014). **(C, top)** Templating approaches in which a matrix is cast around the template. The template is subsequently removed, generating hollow channels, which can be seeded and perfused. **(C, bottom)** Three-dimensional printing (bioprinting) in which vascular and cell inks are used to generate a 3D tissue with embedded, perfusable vascular channels. Reproduced from Ref. (Miller et al., 2012). **(D, top)** ECM-based soft lithography in which microfluidic channels are filled with ECM (Wang et al., 2016). **(D, bottom)** Micrographs of vasculogenic and angiogenic vessel formation in the fibrin matrix as a function of time. Reproduced from Ref. (Kim et al., 2013).

using on-chip microvascular models (Chen et al., 2017) (see Section 2.2 for further details). Remarkably, vascularized OOC are suitable for screening the efficacy/toxicity of libraries of relevant compounds against multiple tissues in a more physiological environment. Finally it is worth mentioning that Pradhan et al. investigated how hemodynamic forces and vascular parenchymal mechanotransduction influences relevant pathways in organ-specific niches and pathophysiological states, a possible way toward developing mechanotherapeutics (Pradhan et al., 2020). A further option is to transfer tissues on chip, where further studies are then carried out.

In terms of bioavailability, blood organ barriers can however limit drugs in reaching their targets. For these reasons, numerous studies focused on the accuracy of microfluidic-based in vitro reproduction of these barriers in order to provide miniaturized and controllable platforms for investigating drug delivery and pharmacokinetics as well as nutrient/gas/waste exchange. The gut and lung cases were described before. Another important case is represented by the blood-brain barrier which is relevant for administering drugs to the brain and for developing therapies for neurodegenerative diseases (see Section 2.1 for details). Other examples of applications to liver and kidney are reported in Section 2.4 since these organs are key players in drug metabolism and clearance with impact on bioabailability and side effects/toxicity.

3. Microphysiological systems for (other) organs/disease studies and multi-organs platforms

3.1. Blood brain barrier and OOC for neurodegenerative diseases

The blood-brain barrier (BBB) separates bloodstream from brain tissue and is formed by specialized endothelial cells, pericytes and astrocytes up to neurons, as illustrated in Fig. 8 top (van der Helm et al., 2016; Osaki et al., 2018b). Its study attracted significant attention as the BBB represents a formidable challenge to access the central nervous system for delivery of pharmaceuticals and therapeutic antibodies against neurological disorders. Indeed, by implementing its neuroprotective function, the BBB tightly regulates transport of biomolecules and harmful compounds. It is characterized by low permeability to most chemical compounds and provides homeostasis for optimal neuronal function (van der Helm et al., 2016). To increase the throughput of present technologies and overcome their limitations, engineered microfluidic BBB models have been proposed. However, they must satisfy a number of criteria: high-fidelity in mimicking in vivo physiological microenvironment and relevant conditions/functions, possibility for investigating organ-level functions, stability for a prolonged period to permit real-time study, recirculating perfusion for drug permeability studies, and of course standardization and reproducibility (van der Helm et al., 2016).

Various proposed BBB-on-a-chip models rely on co-cultures of neurovascular endothelial cells and primary astrocytes on the two sides of a porous membrane (Wang et al., 2017). This approach was shown to better recapitulating in vivo conditions and to result in tighter junctions and lower barrier permeability than the case with only endothelial cells (Jeong et al., 2018). Moreover, it allows recirculation at physiologically relevant perfusion rates and the application of shear stress at in vivo levels. An example of this class of microfluidic BBB models is reproduced in Fig. 8 A1 (Wang et al., 2017) which summarizes all the main components and details of the layout used by Wang et al. for co-cultures of rat primary astrocytes and brain microvascular endothelial cells (BMECs) derived from human induced pluripotent stem cells (hiPSCs). Similarly, Park et al. combined hiPSC-derived human brain microvascular endothelium with primary human brain astrocytes and pericytes (Park et al., 2019). Notably, differentiation under hypoxic conditions enhanced barrier functionality with high levels of tight junction SLC and ABC proteins, functional efflux pumps and surface proteins modulated transcytosis capabilities for drug, peptide, nanoparticle and antibody.

When characterizing barrier-forming tissues, a crucial step is the assessment of barrier integrity and function, which should be maintained in time for the whole duration of the study. For this purpose, various in vitro techniques are available, from microscopy imaging of cell-cell adhesion proteins to measuring ionic currents, to flux of water or transport of molecules across cellular barriers (Arik et al., 2018). In their work, to evaluate barrier integrity, Wang et al. performed time lapse studies by immunostaining for the tight junction proteins, ZO-1 and claudin-5, while cell nuclei are stained in blue with DAPI as shown in Fig. 8 A2 (Wang et al., 2017). Recently, trans-endothelial electrical resistance (TEER) measurements (Fig. 8 A3) are attracting strong attention as an alternative electrical procedure for assessment of tight junction formation and comparison with in vivo conditions in various models including the blood-brain barrier (BBB), gastrointestinal (GI) tract, and pulmonary models (Srinivasan et al., 2015). Notably a tighter barrier was observed when using co-cultures.

To further analyze barrier function, permeability assays are commonly carried out using fluorescent tracers, large molecules (FITC-dextrans) and model drugs (caffeine, cimetidine, and doxorubicin) as well as permeability mediators with results compared with in vivo permeability coefficients values (Wang et al., 2017). In this respect, it is of particular interest an electrochemical permeability assay introduced by Wong et al. as a method to overcome the need for complex optical instrumentation and laborious manual sampling by using an electroactive tracer (Wong and Simmons, 2019).

Not all microfluidic BBB platforms with low permeability have been, however, implemented with the membrane-based approach. For example, Bang et al. established a 3D blood brain barrier model by the direct contact between a perfusable vascular network and astrocytes in an architecture comprising a vascular and a neural channel (Fig. 8 B1–B2) (Bang et al., 2017). These side channels were supplied by different media resulting in better barrier properties and viability with respect to the single medium cases. Notably, the vascular network permeability for FITC-dextrans was estimated to be similar to in vivo values and the authors also observed a good neurovascular interfacing and the presence of synapses.

Beyond facilitating the development of new treatments, the availability of such microfluidic models of tissue barriers can facilitate an improved understanding of their functionality and disruption which are associated to the pathophysiology of many diseases (Arik et al., 2018). For example, Brown et al. used a microfluidic model of the human neurovascular unit to investigate the inflammatory disruption of the blood-brain barrier, its metabolic consequences and repair mechanisms. Namely, a loss of barrier function associated to increased diffusion and reduced presence of tight junctions was observed upon inflammatory stimulation using lipopolysaccharides or a cytokine cocktail to mimic systemic and local infections. Then, the authors demonstrated how metabolite analysis can contribute to identify critical pathways in inflammatory response (Brown et al., 2016). Present limitations in BBB-on-chip field concern standardization of methods for quantification of relevant parameters such as barrier permeability and shear stress, making difficult a direct comparison in terms of performance (van der Helm et al., 2016).

Remarkably, microfluidic neurodegenerative diseases models for both the central and peripheral nervous system focusing on Alzheimer's disease, Parkinson's disease, and amyotrophic lateral sclerosis were implemented recapitulating their critical features with compartmentalized microenvironments for the co-culture of neurons, glial cells, endothelial cells, and skeletal muscle cells and the ability to reproduce chemical gradients and mechanical features (Osaki et al., 2018b).

To summarize, different (vertical) and planar architectures have been implemented with various cell lines co-cultured in order to model the BBB on chip. Other parameters to take into account in the chip design include membranes selection and ECM coating. The incorporation of physiological shear stress, inflammatory stimulation and the integration of sensors for TEER measurements provide advantages with respect to traditional methodologies.

3.2. Tumor models and organoids engineering for new drug development

The development of cancer-on-chip models is of particular interest for their potentials to recapitulate the cancer pathophysiology by reconstructing the highly complex tumor microenvironment (TME) composed by several factors, including extracellular matrix (ECM), blood vasculature, and multiple stromal cells, which control cellular function, proliferation and cancer metastasis.

Conventional in vitro models based on monolayer cultures are unable to accurately mimic the in vivo environment and, consequently, are less effective for drugs research. On the other hand, the use of animal models has limitations for high-throughput screening in preclinical drug testing because of high consumption of chemicals, time consuming operations, constraints in study of the mechanisms at play and species-specific differences. By combining modern microfluidic and tissue engineering technologies, tumors-on-chips (ToC) provide more biomimetic and high-throughput in vitro models. ToC can recapitulate the complex microphysiological features of disease microenvironments by enabling the production of three-dimensional models and replicating tumor and vasculature interactions, tumor angiogenesis and metastasis. As a consequence, they can accelerate drug development and screening.

In this scenario, tumor spheroids/organoids are considered the best

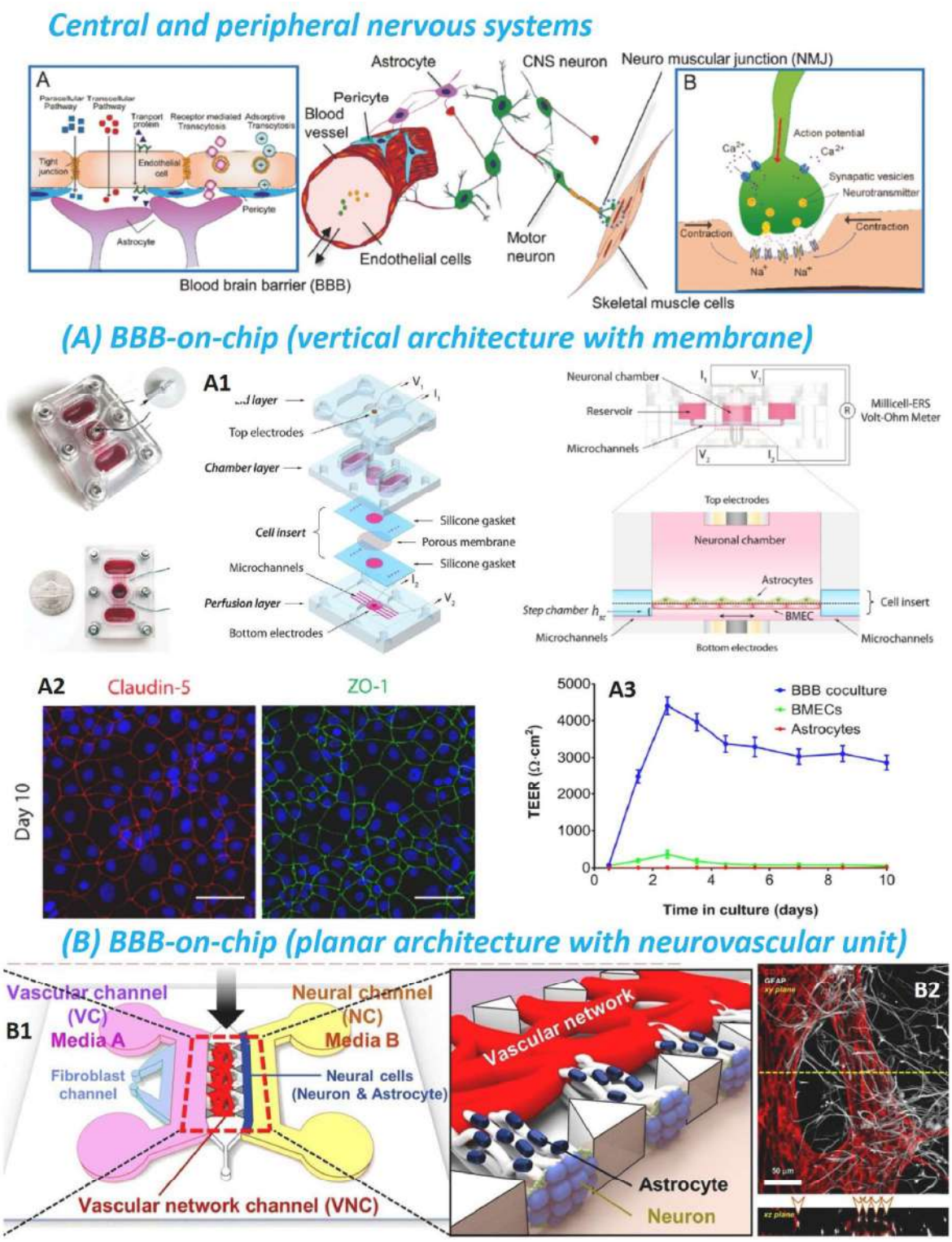

Fig. 8. **(Top)** The main players at the central and peripheral nervous systems (CNS and PNS involved in neurodegenerative diseases (Osaki et al., 2018b). **(top left)** At CNS level, the blood–brain barrier (BBB) separates bloodstream from brain tissue. It is characterized by tight junctions and a very low permeability with access through paracellular and transcellupar pathways. It involves different cell types: endothelial cells, pericytes, astrocytes and CNS neurons. **(top right)** At PNS level, motor neurons and muscle fibers form the neuromuscular junction, which is a chemical synapse. Muscle contraction is driven by signals transmitted by the motor neurons to the muscle in the form of acetylcholine release. Reproduced from Ref. (Osaki et al., 2018b) **(A1)** Vertical structure of the BBB-on-chip reported by Wang et al. and evaluation of barrier integrity **(A2)** by immunostaining for the tight junction proteins Claudin-5 and ZO-1 and **(A3)** by TEER measurements. Reproduced from (Wang et al., 2017); (**B1**) Planar microfluidic platform for neurovascular unit containing blood-brain barrier. **(B2)** Confocal microscopy image of the direct vascular network-astrocyte interface that confirmed direct contact on two axes, with contact points indicated in the xz plane through arrows. Reproduced from (Bang et al., 2017).

models for cancer research. They are self-assembled cancer cells aggregates with diameters from 100 μm to 1000 μm. Tumor spheroid formation attracted significant attention because they are able to better mimic the in vivo TME providing a more accurate platform for cancer investigation and therapeutic testing. Indeed, they are able to reproduce the extracellular matrix environment (ECM), cell–cell interactions and the presence of nutrients, metabolites and oxygen gradients (Kwapiszewska et al., 2014) beyond their 3D structure. Furthermore, they can be produced from a variety of tumor cell lines including human and patient-derived cells.

Conventional homogeneous spheroids formation is achieved with techniques such as hanging drop and rotating flask methods, and the use of external (e.g. electric field or magnetic) forces or non-adhesive surfaces. These techniques allow drug testing and performance analysis, and commercial systems are available on the market, such as Insphero, Aggrewells (Stem Cell Technologies) and Nucleon Sphera (ThermoFisher). However, they require frequent media exchange and are labor-intensive and time consuming. On the other hand, in microfluidic systems, procedures can be automated and the formation of tumor spheroids can be achieved from a small number of cells, with continuous infusion of the culture medium ensuring high cell activity, small sample and reagents volumes. This guarantees high sensitivity and integration, with advantages in terms of arraying the samples and testing various combinatorial treatments with high throughput.

Other studies addressed on chip investigation of tumor and vasculature interactions, tumor angiogenesis and metastasis. Among them, the self-assembly microvascular approach allows to recreate on chip tumor angiogenesis and to emulate metastatic cascade (Mollica et al., 2019) such as invasion/intravasation (Du et al., 2018), extravasion of tumor cell (Chen et al., 2016a, 2017; Song et al., 2018b) and perivascular niche (Xiao et al., 2019; Sobrino et al., 2016b; Phan et al., 2017; Marturano-Kruik et al., 2018). Indeed, typically in a metastatic cascade, first tumor cells invade the blood circulation passing the extracellular matrix and the vascular endothelium. Then cancer cells extravasate at the distant site travelling across the endothelium blood vessel to leave the circulation and colonize another tissue/organ giving rise to a new metastatic TME or secondary tumor formation (Xu et al., 2016; Lim et al., 2021; Zhang et al., 2022; Lin et al., 2020; Del Piccolo et al., 2021; Imparato et al., 2022) (Fig. 9 top).

In this respect, Du et al. (2018) reported a microfluidic co-culture system containing both breast cancer cells (MDA-MB-231) and noncancerous cells (MCF-10A or HDF-n), which was employed to investigate the influence of the tumor microenvironment on metastasis before intravasation into the vessels. A vascular endothelial layer was also recreated in order to mimic the semipermeable membrane function and the transendothelial nutrients transport in blood vessels. The authors demonstrated the ability of the developed tool to study the mechanism of tumor invasion into the stroma and to screen anti-metastatic drugs. Chen et al. (2017) instead presented a microfluidic platform with self-organized perfusable human microvascular networks formed over 4–5 days, after which the tumor was perfused and extravasation events were tracked over 72 h via standard confocal microscopy (Fig. 9 A). This assay allows a rapid quantification of tumor cell extravasation kinetics and can be used for the screening of therapeutic agents. As another example, Xiao. et al. (Xiao et al., 2019) reproduced on-a-chip the microvasculature as a perivascular niche model to evaluate the ex vivo dynamics of brain tumor stem-like cells (BTSCs) derived from glioblastoma patients. They found that the degree of colocalization between tumor cells and microvessels depends on the genetic and pathologic subtypes of the tumor samples and varies significantly across patients. These findings demonstrate the potential of the developed assay for ex vivo analysis of tumor cell dynamics and heterogeneity, representing a new route to study patient-specific tumor cell functions.

As described above, considerable efforts were dedicated to combine tumor cells and microvasculature on chip with the aim to achieve a more in deep understanding on the angiogenesis processes, the interaction of the cancer cells with the microvasculature and the metastasis cascade dynamics. However, the aforementioned models do not recapitulate the pathophysiology of vascularized solid tumor tissue, but it is known that this is a critical feature in cancer treatment. For this reason, novel technologies were developed to culture 3D solid tumor tissue (or tumor spheroids) with microvasculature on-a-chip (Lee et al., 2018a; Chung et al., 2017; Ayuso et al., 2018; Nashimoto et al., 2020; Haase et al., 2020).

In this respect, Nashimoto et al. interconnected a spheroid to a perfusable vascular network inducing angiogenic sprouts from the microchannels up to reaching vessel-like structures in the spheroid (Nashimoto et al., 2017) (Fig. 9 B1). Intriguingly, they demonstrated the presence of a continuous interconnection available to deliver biomolecules and drugs. The constructed vascular network allowed long-term perfusion culture of the tumor spheroids which result in a significant enhancement of the proliferation activities of tumor cells and in a non-conventional dose-dependent response to the anticancer drug, highlighting the importance of vasculature network flow in evaluating tumor activities in a drug screening platform (Nashimoto et al., 2020) (Fig. 9 B2–B4). This achievement allows to mimic in vivo TMEs and represents an important achievement for all the studies on spheroids/organoids/tumoroids. Using a vascularized tumor model based on microtumors arrays with independently-addressable elements, a blinded screen of both anti-cancer and anti-angiogenic drugs was performed by Phan et al. (2017) (Fig. 9 C). Further efforts may be necessary in this direction to develop more powerful tools for fundamental studies in tumor angiogenesis and drug testing targeting a clinical personalized therapeutic treatment.

3.3. *Biomechanical structures - bone-on-a-chip and heart-on-a-chip*

Biomechanical structures represent key components of the human body and include bones, muscles and tendons. Several 2D models for bones and cartilage employ a single type of cells (chondrocytes for the cartilage; osteoblasts, osteocytes, and osteoclasts for the bone) (Hodgkinson et al., 2022) with intrinsic limitations. Another important aspect is that a reliable in vitro model must allow to investigate the influence of mechanical cues. This can be achieved in different ways. An option consists in seeding bone cells on 2D membranes which are pneumatically or electromagnetically deformed to introduce cyclical cell stretching. In microfluidic systems, shear stresses can be recapitulated by means of fluid flow. Among the co-cultures models, it is worth mentioning the work by Middleton and coworkers who investigated osteocyte-osteoclast signaling under shear stress stimulation (Middleton et al., 2017). 3D models were implemented using different scaffold materials, prevalently natural hydrogels (such as collagen, gelatin, hyaluronic acid, alginate) and synthetic polymers (e.g. polyethylene glycol, PNIPAM, PDLLA). The first class presents advantages in terms of biocompatibility, permeability, similarity to natural tissues, presence of motifs for cell adhesion, non- or low-immunogenicity. Furthermore, they are low cost and they properties can be tuned, e.g. by chemical modification (e.g. ECM stiffness is relevant for osteoarthritis pathogenesis and progression (see Section 3.3 for details on Materials for OOC). Bone models were also engineered using hydroxyapatite as a constitutive material resembling bone mineralization products and favourable for proliferation and osteogenic differentiation of the human foetal osteoblast cell line (hFOB) (Tang et al., 2021). In particular, Tang et al. produced hydroxyapatite microfluidic chips by ceramic stereolithography with a diffusive mixer to achieve a concentration gradient of the model drug doxorubicin hydrochloride (DOX) and evaluate its half maximal inhibitory concentration (IC50) (Tang et al., 2021). Hydroxyapatite-based nanocomposites are attractive materials for bone tissue engineering and their cytocompatibility was demonstrated with respect to the MG63 osteoblast-like cell line (Scialla et al., 2017). Recently, vascularized bone-on-chip models attracted attention (Whelan et al., 2021) and a neuro-vascularized bone chip was implemented by

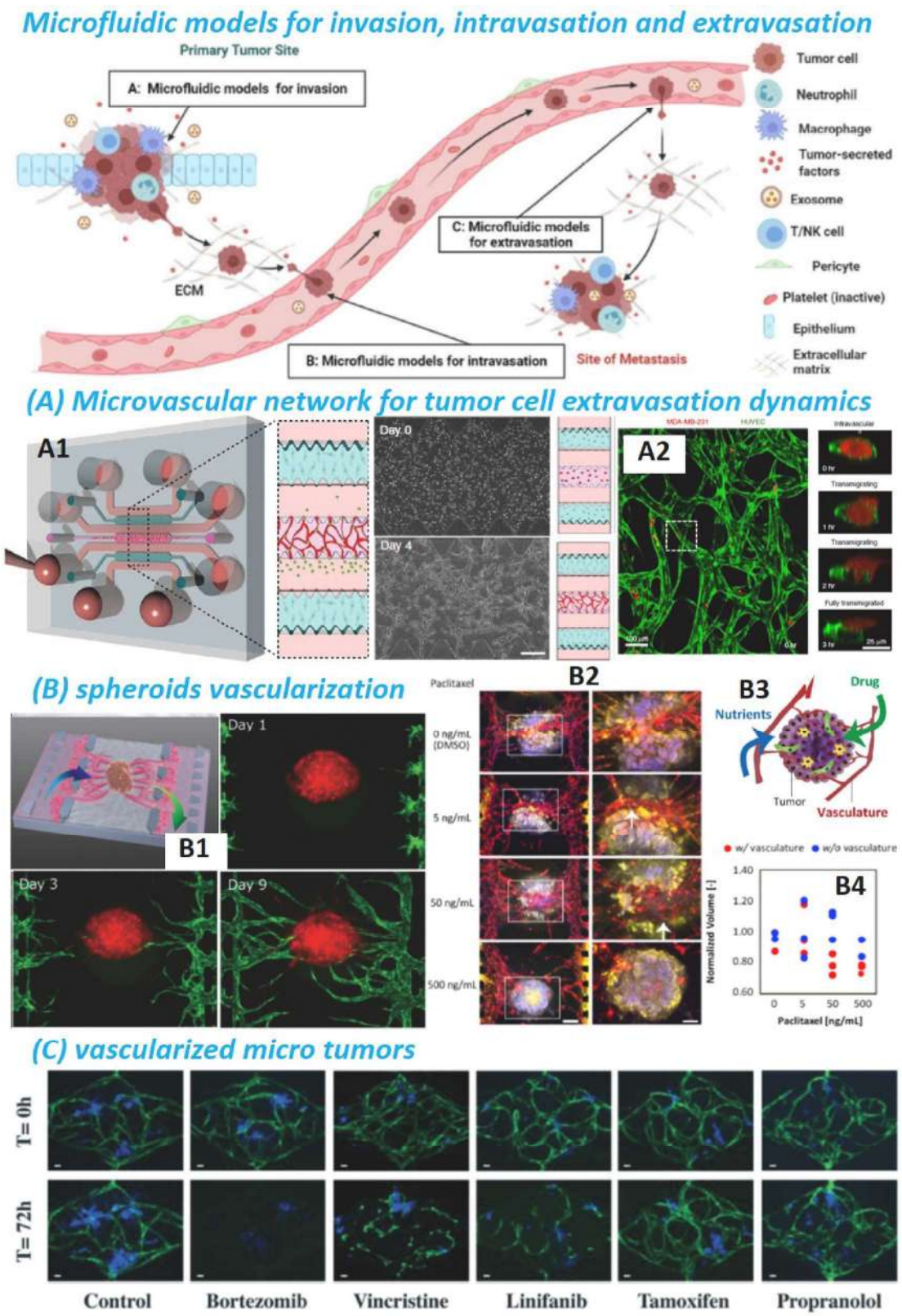

Fig. 9. (Top) *Microfluidic models including metastatic steps from invasion to intravasation and extravasation. Reproduced from Ref.* (Zhang et al., 2022) ***(A1)*** *Microfluidic platform with self-organized perfusable human microvascular networks formed over 4–5 days.* ***(A2)*** *Confocal image of a region of tumor-perfused (red) microvascular network (green) and cross-sectional views of a transmigrating tumor cell (right sequence) with extravasation scoring. Reproduced from Ref.* (Chen et al., 2017). ***(B1)*** *Schematic diagram and fluorescent micrograph of a sferoid interconnected to a perfusable vascular network inducing angiogenic sprouts. Reproduced from Ref.* (Nashimoto et al., 2017). ***(B2)*** *Immunofluorescence images of the tumor spheroid with the vasculature under drug administration at different doses.* ***(B3)*** *Tumor vasculature for nutrients and drugs.* ***(B4)*** *Spheroid volumes as a function of drug concentration calculated from sequential histological sections Reproduced from Ref.* (Nashimoto et al., 2020). ***(C)*** *VMT arrays for drug screening with ECFC-EC formed vascular networks around HCT116 colorectal cancer cells and evaluation of drug efficacy on tumor growth and the associated vasculature quantified after 72 h (reproduced from* (Phan et al., 2017)*).*

Neto et al. with three channels comprising nerve, vascular and bone unit in order to investigate the response to inflammatory bone conditions and its effect first on the vascular unit and then on the nerve unit (Neto et al., 2102) (Fig. 10 A1-A2). This platform can provide a useful tool for drug development and the authors investigated anti-inflammatory drug nanodelivery by means of nanoparticles. In another study, bone regeneration was also studied on chip (Galvan-Chacon et al., 1002).

Muscles are the other major biomechanical structures beyond bones. In this respect, heart-on-a-chip models assume particular relevance since cardiac pathologies have high impact on worldwide morbidity and mortality rates. Furthermore, there is a high incidence of cardiovascular drug toxicity combined with the severity of adverse drug reactions in late-stage drug development (Savoji et al., 2019). For these reasons, human heart muscle on chip models have been developed to mimic healthy and pathological cardiac tissues and provide high-throughput tools alternative to animal models for testing cardiovascular drugs, cardiotoxicity and cardioprotective efficacy in preclinical trials (Meyer et al., 2019). In these studies, the cardiac/myocardial mechanics and heart muscle contractility are central indicators and contractile force development can be a phenotyping issue in cardiomyocyte-on-a-chip models (Meyer et al., 2019). Microcantilevers are a hallmark of cardiac OOC. In a pioneering work, Legant et al. reported 3D myotubes attached to MEMS microcantilevers as tissue gauges to measure the microtissue-generated forces (Legant et al., 2009). Few years later, Agarwal et al. recapitulated heart ventricle architecture on flexible cantilevers of soft elastomers, whose deflection was used to evaluate the generated diastolic and systolic stresses (Agarwal et al., 2013). The integration of flexible strain gauge sensors is a characteristics of the architecture from Parker group to monitor the contractile stress and beat rate of the reconstituted cardiac tissue (Lind et al., 2017a) and how they are influenced by administration of bioactive compounds and drugs (see also Section 3.2 for discussion on sensors for OOC). The addition of endothelial barrier model then permitted them to test the delivery through the blood vessels toward heart musculature (Lind et al., 2017b). A dose–response analysis on the effect of 12 cardiac and cardiotoxic drugs was instead carried out on a model of the ventricle laminar structure reconstituted by Lind et al. using cardiomyocytes derived by human induced pluripotent stem cells (Lind et al., 2017b). In a recent

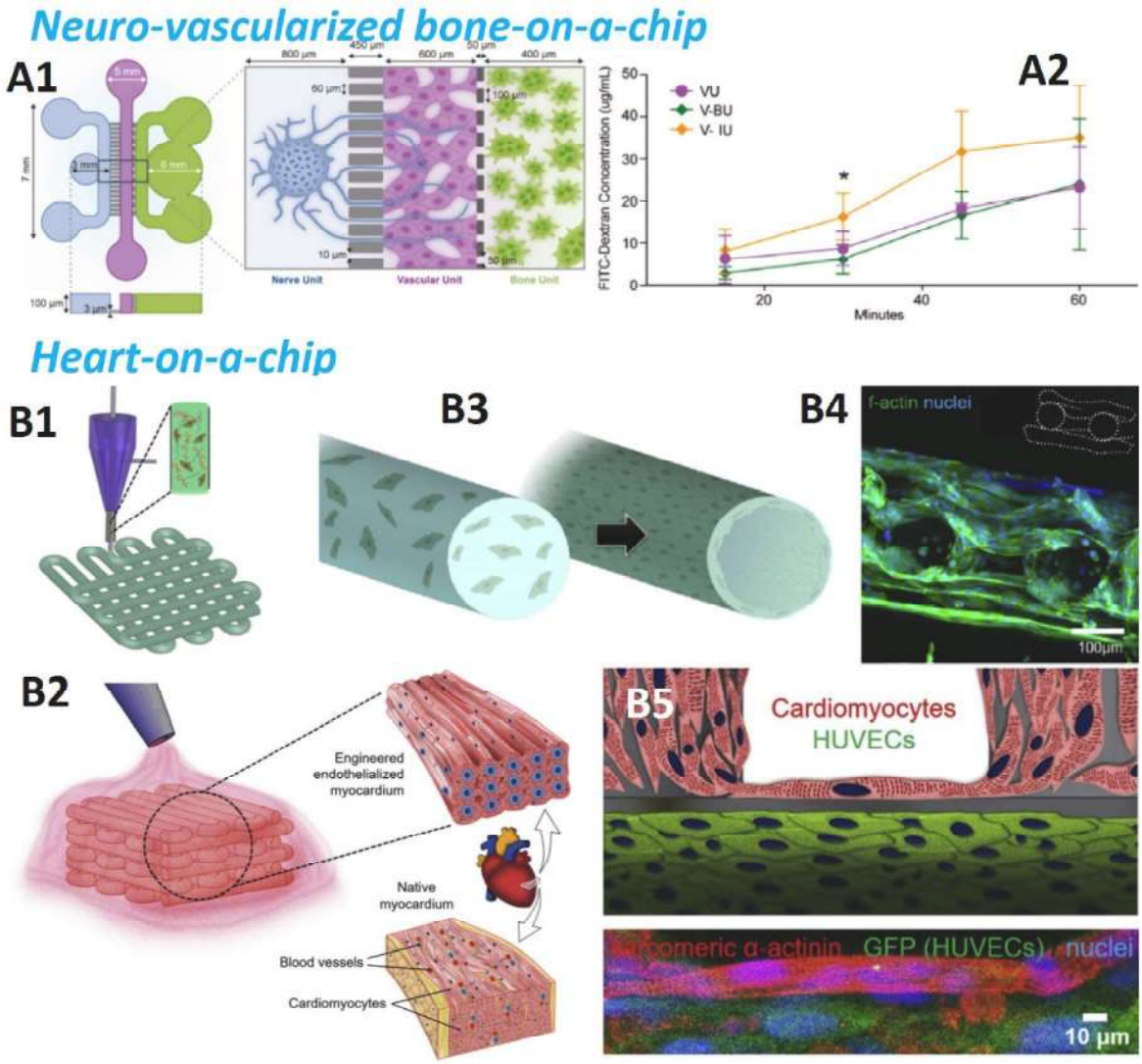

Fig. 10. **(A1)** *Model of neuro-vascularized bone chip. Reproduced from Ref.* (Neto et al., 2102). ***(A2)*** *Permeability of the endothelial barrier evaluated at the vascular unit adjacent to the bone inflammatory unit (V-IU)—osteoclasts under IL-1β exposure—and compared to vascular unit adjacent to the physiological bone unit (V-BU)—osteoclasts in standard culture conditions.* ***(B1–B2)*** *Schematic diagrams of the process for fabricating endothelialized myocardium by 3D bioprinting.* ***(B3)*** *Schematics of the assembly of human umbilical vein endothelial cells encapsulated in bioprinted microfibers into a layer of endothelium.* ***(B4)*** *Confocal fluorescence micrograph indicating the formation of the endothelium by human umbilical vein endothelial cells.* ***(B5)*** *Schematic and confocal fluorescence images of an endothelialized myocardial tissue realized by seeding neonatal rat cardiomyocytes on to the bioprinted endothelialized microfibrous scaffold. Reproduced from Ref.* (Zhang et al., 2016).

work, Ren et al. validated the maturation and phenotypic changes of cardiomyocytes cultured in well-aligned structures and successfully reproduced their synchronous beating upon electrical pulse stimulations (Ren et al., 2020). DOX-induced cardiotoxicity and the cardioprotective efficacy of CAR and IVA drugs were then assessed.

In terms of real time monitoring, transepithelial electrical resistance (TEER) sensors and multi-electrode arrays (MEAs) were used for evaluating tissue barrier function and recording cardiac activities (see Section 3.2) (Maoz et al., 2017). Photonic crystals provided alternative self-reporting monitoring tools of cardiomyocytes activity (Shang et al., 2020). Furthermore, bioprinting is starting to have a significant impact on the field. Indeed, Zhang et al. fabricated endothelialized myocardium model capable of spontaneous and synchronous contraction by printing endothelial cells within microfibrous hydrogel scaffolds and then seeding cardiomyocytes (Zhang et al., 2016) (Fig. 10 B1–B5). An aorta smooth muscle-on-a-chip was implemented by Abudupataer and coworkers (Abudupataer et al., 2021).

A further target for of large interest is represented by OOC models for amyotrophic lateral sclerosis (ALS) and neuromuscular development and disease which were developed combining human iPS-derived muscle cells and optogenetic motor neurons (Osaki et al., 2018c; Arjmand et al., 2022; Fralish et al., 2021). However, they are not discussed here for space constraints. In general, mechanobiology and mechanotransduction attracted large interest for the relevance in many biological processes. For this reason, biomechanical aspects have been also investigated in lungs and gut as discussed above (e.g. simulating breath and peristaltic stimuli). In this respect, OOC platforms provide advanced tools for investigation under well controlled and engineered conditions.

3.4. Metabolism-on-chip – liver, kidney and multi-organ models

Beyond the intestine, liver, kidney and pancreas on chip models were investigated. They are relevant for considering the role of drug metabolism/clearance beyond absorption, as well as for assessing potential organ damage and for evaluating multi-organ interactions (see Section 2.5) (Bovard et al., 2018; Maschmeyer et al., 2015a; De Gregorio et al., 2020; Foster et al., 2019; Christoffersson et al., 2019; Tan et al., 2019; Decsi et al., 2019; Deng et al., 2019; Theobald et al., 2018, 2019; Lee and Sung, 2018; Ong et al., 2019; Vernetti et al., 2017; Bavli et al., 2016; No et al., 2015; Bale et al., 2014; Esch et al., 2014; Shintu et al., 2012a; Zhang et al., 2009; Fabre et al., 2020; Phillips et al., 2020; Peel et al., 2019; Musah et al., 2017a, 2018; Wilmer et al., 2016; Jang et al., 2013; Miller and Shuler, 2016a).

3.4.1. Liver-on-a-chip

The liver is responsible for various functions including the production of bile, serum proteins (albumin), and lipoproteins, and it has a key role in the metabolism of amino acids, lipids, and carbohydrates taken with food. It is also involved in the detoxification process of endogenous (bilirubin) and exogenous products such as drugs. The detoxification process can lead to drug-induced liver injury (DILI). Animal models and in vitro cell culture models were used to evaluate drug-induced damage to the liver. However, due to the species-specific differences that exist between animals and humans and due to the low sensitivity of in vitro models, neither type has led to good results in the prediction of DILI (Ware and Khetani, 2017; Jang et al., 2019). In this respect, Organ-on chips (OOC) can again provide useful tools to mimic the functional and structural unity of the liver, including physical and chemical stimuli (Gough et al., 2021).

A multispecies liver-on-chip could be helpful to understand toxicities detected in animal models in order to better determine human safety. For this reason, Jang et al. (2019) realized a liver-on-chip to study the different types of toxicity in the liver of dogs, rats, and humans when they are treated with different drugs. Their chip was composed of a top parenchymal channel, where primary rat, dog or human hepatocytes were seeded on a porous ECM (extracellular matrix)-coated membrane. Then in the bottom vascular channel below the membrane, sinusoidal endothelial cells (LSEC), Kupffer cells and stellate cells were seeded (Fig. 11 A). To verify if this liver-on-chip could be helpful to predict species-specific DILI responses, the authors evaluated the hepatotoxic effects caused by bosentan, an endothelin receptor antagonist vasodilator, that induces cholestasis in humans but not in dogs or rats, using the three species models. As shown in Fig. 11 B, the administration of Bosentan at 1, 10 and 100 μM led to a decrease in albumin secretion in dog and human chips but not in rat chip. Moreover, the plasma concentration of bosentan that has been associated with DILI in humans is similar to the concentration in the human liver-chip at which they observed toxicity. The chip was also more sensitive compared to culture plates and this could be due to the presence of a fluid flow and better hepatocyte functionality. In another study, Jang et al. studied the toxic effect caused to the liver by the generic analgesic acetaminophen (APAP), which through its toxic and reactive metabolite N-acetyl-p-benzoquinone exhausts cellular glutathione and leads to oxidative stress in the cells. This process was observed through a cellROX fluorescent probe that binds to reactive oxygen species (Jang et al., 2019).

Hepatotoxicity tests were performed by Bircsak et al. (2021) using a multiwell microfluidic plate, Mimetas OrganoPlate® 2-lane (Fig. 11 C). In this case, the liver-on-chip is present in OrganoPlate 2-lane and consists of an organ channel where they seeded clusters of pluripotent stem cell (iPSC)- derived hepatocytes (iHep) on an extracellular matrix, and a perfusion channel where they seeded HMEC-1 endothelial cells and differentiated THP-1 into macrophages. Cells were shown to remain viable for 15 days by secretome measurements (albumin and urea secretion) and image-based analysis. To demonstrate ability to discover hepatotoxicity, the authors treated the cells with troglitazone (180μ M) as a hepatotoxin for positive control, and 0.5% dimethyl sulfoxide (DMSO) as vehicle control. Then, similar conditions with 72 h exposure time and the same assays were employed to validate the liver toxicity of a library of 159 compounds by means of a Toxicological Prioritization Index (ToxPi score), which is a dimensionless weighted linear combination of %live iHep, urea, iHep nuclear size and albumin. Among 159 compounds, 39 were found to be toxic and 34 of them showed a decrease in iHep viability compared to vehicle control (DMSO). Then, for dose-response evaluation, the authors considered 21 compounds from the previous screening and these studies confirmed all true negative and true positive compounds, except hyproniazide. These results suggest that the liver-on-chip created in the OrganPlate detects the hepatotoxicity of most compounds and it is possible to perform more chronic exposure analysis with this platform using several time points and additional readings (Bircsak et al., 2021).

Another intriguing study by Tsamandouras et al. (2017) described hepatic drug metabolism changes in the human population using physiological microsystems with hepatocytes taken from different donors. For each donor, they analyzed the metabolic depletion profiles of six different drugs and confirmed that there is an inter-donor variability by comparing the expression levels of metabolism-related genes and other liver functions. Notably, TEER measurements and pH changes of HepG2 hepatoma cell line using a chip-embedded non-toxic sensor were employed by Farooqui et al. (Farooqi et al., 2021) for monitoring drug toxicity on cells exposed to various concentrations of drugs such as doxorubicin, epirubicin and lapatinib. Using this liver-on-chip, the authors demonstrated ability to provide real-time data on drug-induced liver injury in vitro (Fig. 11 D).

3.4.2. Kidney-on-a-chip

The kidneys have the task of filtering metabolic waste products from the blood and expelling them through the urine. Through their functional unit, the nephron, the kidneys maintain the correct hydro-saline balance in the body. Furthermore, they play a key role in drug elimination and therefore may be susceptible to drug-induced nephrotoxicity, which can lead to acute or chronic kidney injuries (Li et al., 2017; Cohen et al., 2021). Drugs that can cause nephrotoxicity include antimicrobial,

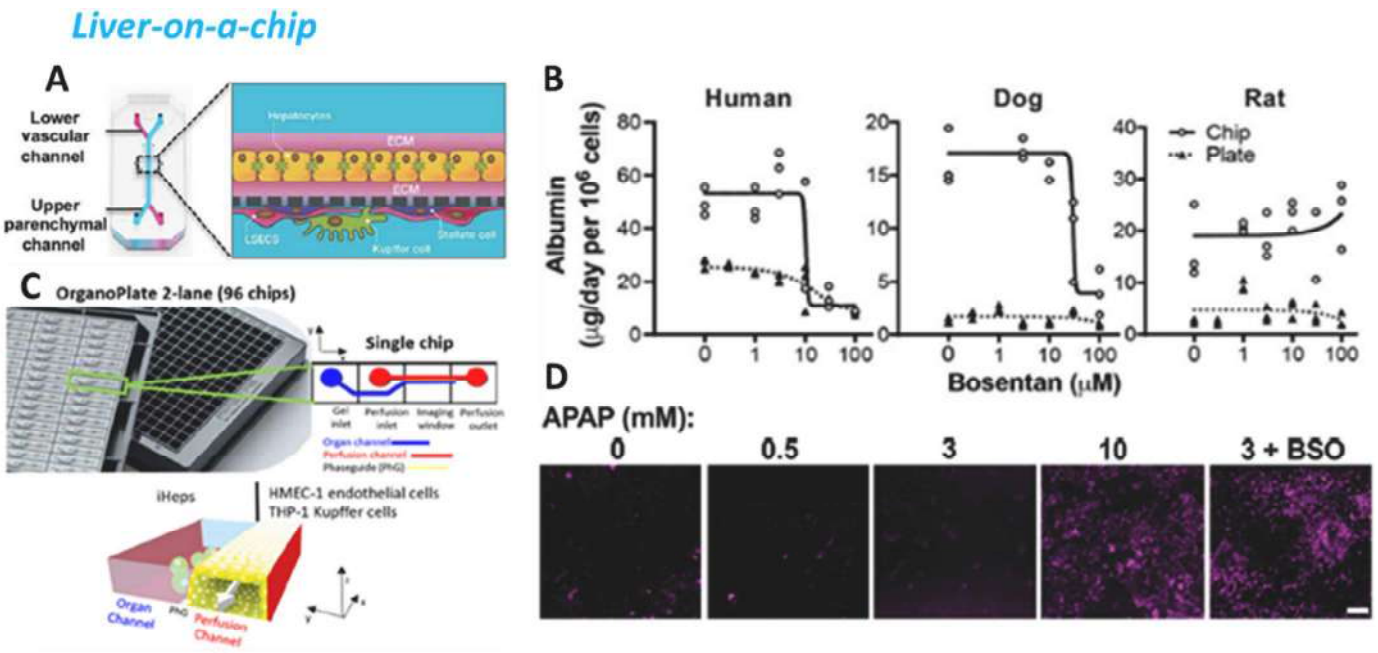

Fig. 11. Liver-on-chip. (A) Liver-on-chip diagram showing which hepatocytes are seeded in the upper channel and Kupffer cells, Stellate cells and LSEC are seeded in the bottom channel. Reproduced from Ref. (Jang et al., 2019). **(B)** Species-specific drug-toxicities in a rat, dog and human liver-chip. Albumin secretion after daily administration of Bosentan at 1,3,10, 30 and 100 μM for 3 days in human chips with two kinds of cells (hepatocyte and LSEC), and plates only with hepatocyte monoculture, and for 7 days in dual-cell dog and rat chips and plates. Reproduced from Ref. (Jang et al., 2019). **(C)** OrganPlate 2-lane. Image of OrganPlate 2-lane with 96 chips and schemes of organ channel and perfusion channel separated by a phaseguide(PHG). Reproduced from Ref. (Bircsak et al., 2021). **(D)** Detection of liver injury caused by acetaminophen(APAP). Images of ROS intensity after daily administration of APAP at 0.5, 3 and 10 mM in human chips. Reproduced from Ref. Jang et al. (2019).

chemotherapeutic, immunosuppressive and analgesic agents (Perazella, 2009). Organ-on–chip (OOC) technology can provide useful tools to reduce the nephrotoxic potential of novel drugs by mimicking organ functions and the complexity of the native tissue better than animal models and 2D culture models due to the presence of a fluid flow, pressure and a co-culture of various types of cells (Ashammakhi et al., 2018).

For example, Yin et al. (2020) employed a kidney-on-chip model to evaluate nephrotoxicity induced by some nephrotoxic drugs such as cisplatin (DDP), gentamycin (GM) and cyclosporin A (CsA). Specifically, they developed a microfluidic platform, where renal proximal tubule epithelial cells (RPTEC) were seeded in the upper layer on a polycarbonate (PC) membrane coated with extracellular matrix (ECM) collagen, while peritubular capillary endothelial cells (PCECS) were seeded in the bottom layer on another PC membrane coated with ECM collagen (Fig. 12 A-B). Their configuration comprised a peristaltic pump that controls the flow rate of the cell culture medium into the chip, a temperature control to maintain an optimal culture medium temperature and matching catheters. The effects of different concentrations of DDP, GM and CsA were evaluated on the kidney-on-chip and compared with results from the Petri dishes (in static condition) with a live/dead assay and a cell counting kit-8 (CCK-8) (Fig. 12 C). Remarkably, Yin et al. demonstrated that the number of live cells was higher in the fluidic condition of the chip than in the static group proving that the microfluidic system can be used for long-term cell culture and nephrotoxic drug screening (Fig. 12 D) (Yin et al., 2020).

In another study, Vormann et al. (2021) used three-lane OrganPlate, purchased by Mimetas, to create a 3D microfluidic platform for the detection of drug-induced kidney injury (DIKI) in the development of new drugs (Fig. 12 E-F). This platform presents: (i) an upper perfusion channel, where they seeded the human primary renal proximal tubule epithelial cells (RPTEC) and human immortalized proximal tubular epithelial cells with organic anion transporter 1 (CiPTEC-OAT1), (ii) a central channel loaded with extracellular matrix gel composed of collagen I and (iii) a bottom perfusion channel where culture medium was added. The channels were divided by structures called Phaseguide that work like pressure barriers. Afterwards, the cells were subjected to a treatment with four nephrotoxic compounds (tenofovir, cyclosporin A, tobramycin and cisplatin) and various assays were carried out to verify the damaging effect of these drugs on the kidney. Cell viability was determined with the cell counting kit-8; instead membrane integrity was observed with lactate dehydrogenase (LDH) activity and with the β-N-acetylglucosaminidase (NAG) – assay kit. They also evaluated gene expression of toxicity and nephrotoxicity markers and performed detection of miRNA in medium cell culture and drug transporter assays. After having chosen certain concentrations of nephrotoxic compounds, these have been shown to cause a decrease in Ci PTEC-OAT1 cell viability and an increased release of LDH for tobramycin and cyclosporin A at the highest concentration tested. With the same concentrations of nephrotoxic compounds administered to the RPETC, reduced cell viability was instead seen only after exposure to tobramycin, thus resulting in the RPETC being less sensitive than the CiPTEC-OAT1 (Vormann et al., 2021).

In ref. Kim et al. (2016), Kim et al. demonstrated the nephrotoxic effects of the antibiotic gentamicin with cell injury markers, such as cell viability and membrane permeability, and they also compared the nephrotoxicity of the gentamicin, using different systems that simulate the pharmacokinetics of continuous infusion and bolus injection in humans. Of the two systems, the one that causes less nephrotoxicity is the one that mimics a once-daily bolus injection. This approach could be used in a large range of drug-induced nephrotoxicity studies. Other researchers used the kidney-on-chip approach to demonstrate the non-toxicity of a compound. For example, the microfluidic platform in ref. (Li and Tian, 2018a) presented human embryonic kidney cells encapsulated in gelatin methacryloyl (GelMA) to simulate the microenvironment and the main functions of the kidney. By administering 30 μM of kaempferol to the embryonic kidney cells for 12h, Li et al. did not notice any cell damage thus demonstrating the non-toxicity of

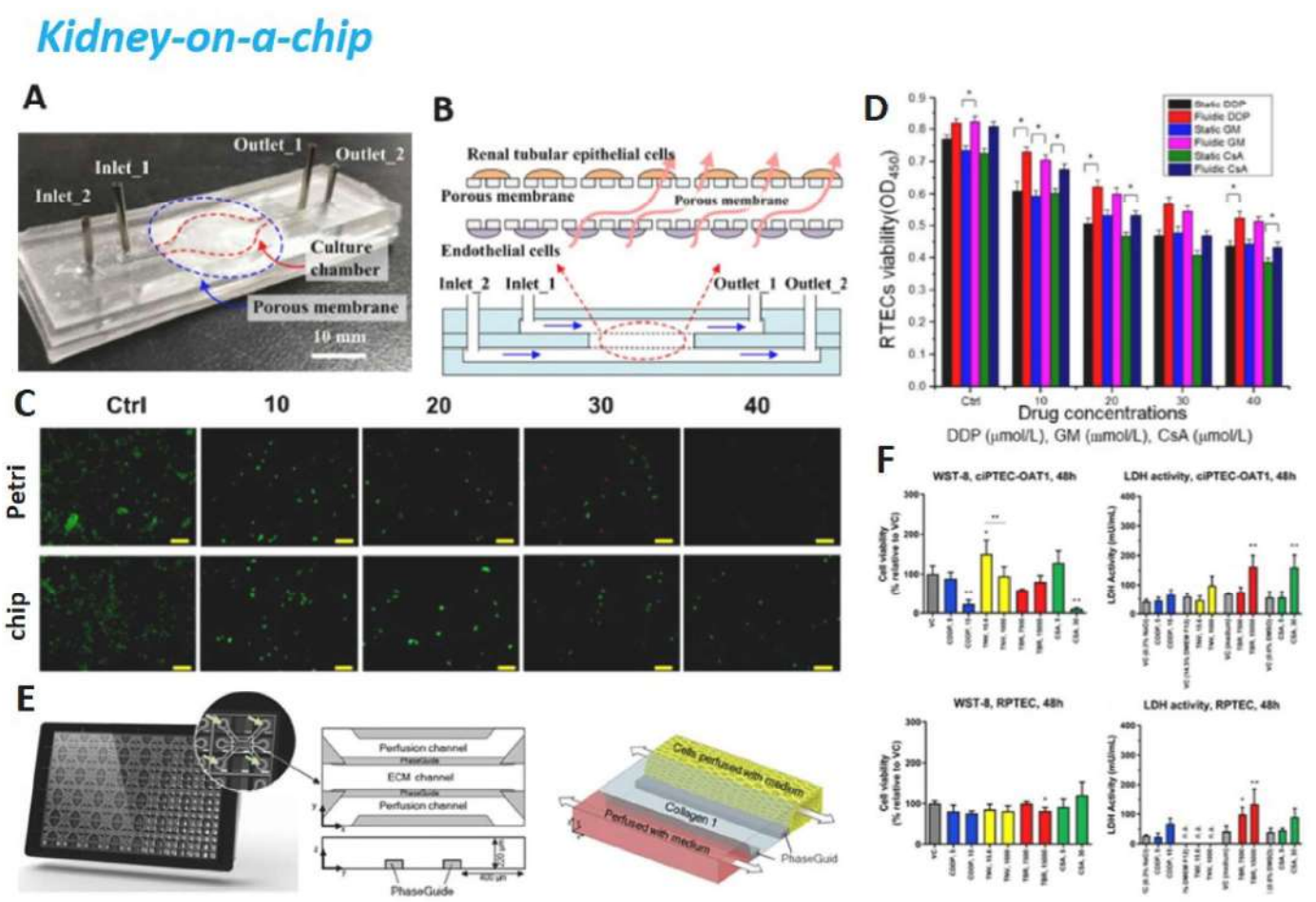

Fig. 12. (A–B) Image and scheme of a microfluidic kidney-on-chip made of three PDMS layers, two membranes, two inlets and two outlets. Reproduced from Ref. (Yin et al., 2020). **(C)** Live/dead cells (RPTECs) assay: live and dead cells (RPTECs) were labelled in green and red respectively. They used different concentrations (10,20,30 and 40 μmol/L) of DDP, under static conditions on Petri dishes and fluidic conditions on chip. Reproduced from Ref. (Yin et al., 2020). **(D)** Statistical analysis: CCK-8 of DDP, GM and CsA under static and fluidic conditions using a microplate reader (*p < 0.05, **p < 0.01). Reproduced from Ref. (Yin et al., 2020). **(E)** Scheme of the Mimetas kidney-on-chip. **(F)** Release of LDH and cell viability upon exposure to model nephrotoxicants cisplatin(CDDP), Tenofovir (TNV), Tobramycin (TBR) and Cyclosporin A (CSA) in RPTEC and in ciPTEC-OAT1 after 48 h *p < 0.05, **p < 0.01. Reproduced from Ref. (Vormann et al., 2021).

kaempferol, a bioactive metabolite from spearmint.

3.5. Multi-organs on chip platforms

Multiple organs on chip platforms (MOC) are the ultimate frontier in OOC research where different organs compartments are interconnected into miniature 'body-on-a-chip' microphysiological systems (MPS). The ambition is to recapitulate organ-organ interaction/crosstalk, physiological relations, methabolic pathways, significant biological barriers and whole-body drug response with an in vivo-like sequential organ-to-organ transfer of media. Intestine models account for absorption and metabolism of drugs, liver for their metabolism and kidney for clearance/excretion to enable a more appropriate evaluation of systemic effectiveness, accuracy and safety of drugs (Maschmeyer et al., 2015b). In this section, we describe this research keeping the focus on drug development from oral-administered (in digestion-on-chip) to inhaled (e.g. lung/liver models) and transdermal-administered drugs (integrating skin). Then some examples of MOC platforms for assessing drug availability and cytotoxicity on tumors, brain and heart are discussed, including applications for brain metastasis studies.

The bioavailability of two orally-administered small molecules (omeprazole and verapamil) was analyzed by de Haan et al. (de Haan et al., 2021). Specifically, the authors employed a three-stages compartmentalized chip to mimic the digestion chain representing mouth, stomach and intestine. For this purpose, three y-shaped micromixers were connected in series adding sequentially saliva, gastric juice and intestinal juice to the previously-treated sample. Finally, the output chime and an additional cell culture matrix were inputted in a fourth micromixer, whose outlet was connected to a flow-through transwell that contains a co-culture of human colorectal adenocarcinoma cell line (Caco-2) and human colon adenocarcinoma mucus-secreting cell line (HT29-MTX-E12). Mass spectrometry (MS) was used for analysis. By means of this flow-based digestion-on-chip, the break down of omeprazole upon exposure to gastric acid was observed, while it arrives undamaged at the cell barrier if added in a way that emulates an enteric lining. Conversely, verapamil was not affected by digestion. A decreased absorption of verapamil was also noted when dissolved in apple juice as matrix (de Haan et al., 2021).

Toxicity studies on inhaled substances were instead the target for Bovard et al. (2018), who combined lung and liver on a chip consisting of a fluidic plate and a reservoir made of polyetheretherketone (PEEK), a nonabsorbent material for small molecules. In the lung compartment, normal human bronchial epithelial (NHBE) cells were cultured at the air-liquid interface (ALI), while the liver compartment consisted of HepaRG liver spheroids. The aim was to mimic the human physiological response that occurs upon inhalation of substances, which are metabolized by both lung and liver CYP enzymes. In presence of liver spheroids, aflatoxin B1 (AFB1) toxicity decreased compared to NHBE lung cells

alone due to crosstalk between the two cell types. Thus such lung/liver MOC platform may be useful for evaluating the toxicity of new inhaled drugs used in the treatment of lung diseases (Bovard et al., 2018). Both inhalation- and intravenous administration were instead the target of comparison in terms of effectiveness and potentially toxicity in the study by Miller and coworkers, whose multi-organ platform integrated lung (including ALI), liver and breast cancer in a single chip (Miller et al., 2020). The cultured cell lines were A549 for the lung, HepG2 C3A for the

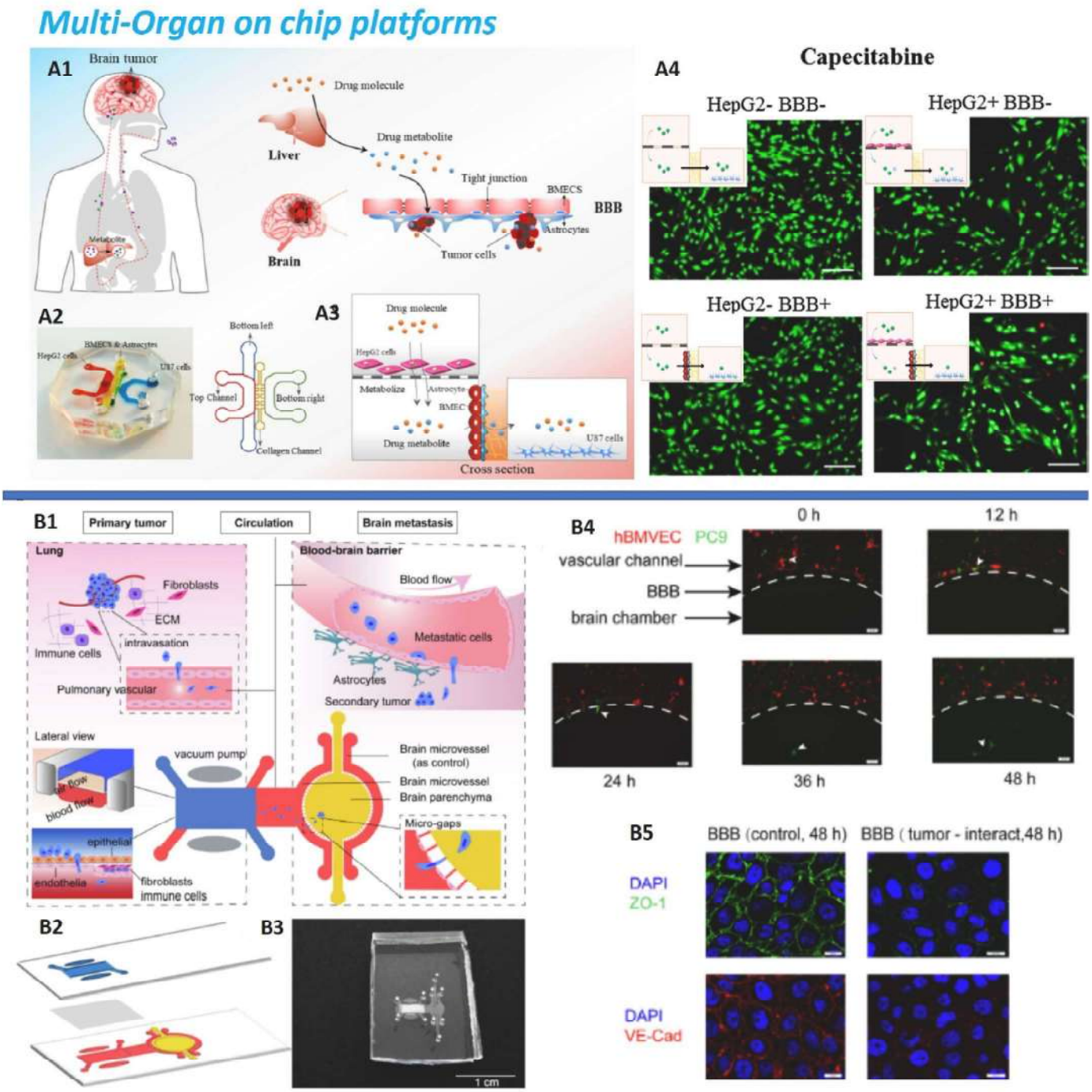

Fig. 13. **(A)** Multi organ-on-chip (liver and brain) platform: **(A1)** Pathway for oral drugs administration to brain tumors through liver metabolic activity and across the BBB. **(A2)** The MOC assembled by Li et al. to recapitulate this process using HepG2 cells in the top (liver) channel, brain microvascular endothelial cells (BMECS) and cerebral astrocytes in the bottom left and U87 cells in bottom right channels. **(A3)** MOC cross-sectional view. **(A4)** U87 cell viability in presence/absence of the liver compartment and the BBB upon administration of 80 μM CAP for 2 days. Live cells stained green, dead cells in red. Bar: 50 μm. Reproduced from Ref. (Li et al., 2021). **(B)** MOC device for the investigation of lung cancer-derived brain metastasis. **(B1)** Pathological process and its recapitulation on chip by Liu et al. (Liu et al., 2019a) through an upstream lung and downstream brain compartment. **(B2)** Structure of the MOC consisting of two PDMS layers and a membrane and **(B3)** its realization, scale bar 1 cm. **(B4)** Extravasation of PC9 lung cancer cells (green) through the BBB (red) in time-lapse images; scale bar, 50 μm. **(B5)** Confocal imaging of the expression of the tight junction zonal occludin-1 (ZO-1, green) and vascular endothelial -cadherin(VE-Cad, red) proteins in the control BBB (left) and in the BBB after tumor cells extravasation (right), evidencing a decrease in tightness upon vascular interaction with tumor cells; Scale bar, 20 μm. Reproduced from Ref. (Liu et al., 2019a).

liver, and MDA MB231 for breast cancer, while curcumin, a natural compound from plants of the Curcuma longa species, represented the investigated drug. Inhalation therapy has the potential to be more economical if applied at home by the patient in contrast to intravenous therapy needing access to a clinical setting. Furthermore, for the same reason, it can be administered more frequently using lower drug level, as a way to reduce toxicity. In their study, the authors emphasized the importance of recirculating flow for more appropriate MOC platform and reported a small influence of curcumin administration on lung and liver viability while its effect was higher on breast cancer cells.

In order to better testing systemic transdermal administration and subsequent drug metabolism, skin models were also integrated in multi-organ-chip. Marx group pioneered this field and in a first study realized a MPS combining skins with liver (Wagner et al., 2013a). Successively, they improved this platform merging skin (with an air–liquid interface), reconstructed human intestinal barrier, liver (spheroids), kidney (in the form of a membrane covered by human proximal tubule epithelial cells) and vasculature mimicked with endothelial cells (Maschmeyer et al., 2015a, 2015b).

Multi-organ platforms have been also realized for predicting anti-tumor drug response. In the case of brain cancer treatments, in addition to the liver involved in drug metabolism, a key role is played by the blood-brain barrier, which selectively regulates the passage of chemicals to and from the brain. As an example, Li et al. (2021) developed a multi-organ device to evaluate how the BBB and liver metabolism influence the availability and cytotoxicity of drugs used to treat glioblastoma (Fig. 13A). Their biomimetic liver-brain chip consisted of microfluidic channels to create three compartments: the left one with human hepatocarcinoma cells (Hepg2) to mimic the liver, the right one with U87 cell to account for the glioblastoma. In between, a porous membrane and type I collagen were placed and rat brain microvascular endothelial cells (BMECS) and astrocytes were co-cultured to recapitulate the BBB. In this way, the chip recapitulated the drug pathway to reach both the liver and the brain upon oral administration. The brain-blood interface was characterized by TEER measurements and through the expression of proteins that constitute occluding junctions, such as ZO-1. Three anticancer drugs were tested in this study, namely Capecitabine, Temozolomide and Paclitaxel. Liver metabolism had limited effect on Temozolomide while resulted in a 30% enhancement of the Capecitabine cytotoxicity on U87 cells. The BBB instead reduced Paclitaxel cytotoxicity by 20%, but Temozolomide and Capecitabine effects were not significantly influenced. In conclusion, this chip allowed to evaluate how the efficacy of a drug targeting the brain is affected by both liver metabolism and the ability to cross the blood-brain barrier (Li et al., 2021).

A similar multi organ on-chip architecture was realized to assess the cardiac safety of an antidepressant drug (clomipramine) which is first metabolized by the liver. After administering 1 μM of drug in an upper compartment containing liver organoids, Yin et al. observed a reduced cell viability and an increased cardiocytotoxicity in the cardiac organoids located in the lower compartment (Yin et al., 2021). Clomipramine also caused a reduction in intracellular calcium flux in the cardiac organoids monitored through a fluorescent Ca^{2+} indicator dye (Fluo-4 AM). Thus, the multi-organ chip permitted to predict the drug side effects both at the level of the main organ involved in its metabolism (the liver) and at the level of the target organ, in this case the heart.

Coming back to cancer, metastasis formation is a key aspect to be addressed. It was discussed in Section 2.2 in terms of interaction of cancer cells with the microvasculature. However, multi-organ models can contribute to gain further insight on the process. Liu et al. (2019a) implemented a platform for studying brain metastasis (BM) from primary tumor growth to its spreading by integrating an upstream lung compartment and a downstream brain including a functional BBB. In Fig. 13B, the metastatic process and the MOC platform are illustrated. The lung model encompassed bronchial epithelial cells, fibroblasts, immune cells, pulmonary vascular endothelial cells, and tumor cells, and employed vacuum channels to account for breathing movements reconstituting the tumorigenesis and cancer intravasation. The brain model consisted of a brain parenchyma chamber surrounded by two vascular channels: (1) the left one connected to the upstream chamber in order to provide a pathway for metastatic cells, (2) the right one unconnected as a control. For cell co-culturing and tumor extravasation, the brain parenchyma compartment was interconnected to the vascular channels by micro-gaps. In their systematic study, the authors employed lung cancer cell lines with differing metastatic abilities and identified the Aldo-keto reductase protein family 1 B10 as a diagnostic biomarker showing higher expression in case of lung cancer BM and a prospective therapeutic target if silenced to limit BBB extravasation.

In order to account for drug absorption, metabolism and clearance, Vernetti et al. reported a five organs platform including jejunum, liver and kidney models (respectively) in addition to skeletal muscle and neurovascular models (Vernetti et al., 2017). The authors observed an organ-specific processing consistent with clinical data in their study of terfenadine for pharmacokinetics and toxicity; trimethylamine (TMA) as a potentially toxic microbiome metabolite; and vitamin D3. Furthermore, trimethylamine-N-oxide (TMAO) resulted able to cross the BBB. Co-culturing endothelial cells, fibroblasts and pericytes with (circulating) immune cells was also considered to investigate immune responses and its influence on disease progression and drug-induced response within an in-vivo mimicking microenvironment (van Dijk et al., 2020; Sun et al., 2019). The microbiota-gut-brain axis attracted large interest too (Raimondi et al., 2019, 2020).

4. Technologies and materials for organs-on-chips

4.1. Microfluidic tools for organs-on-chips and drug research

A number of microfluidic tools have been optimized for Organs-on-Chips. A paradigmatic example concerns application to cancer field, where most of the tools were employed, from vascularization techniques and perfusable channels to administer nutrients and drugs (already discussed in Section 1.4) to microwell arrays, gradient generators and droplet microfluidics (described here). Thus we will draw this section by discussing the main microfluidic components to facilitate high-throughput drug screening with focus on the exemplary case of anti-cancer drug research.

In particular, we can distinguish systems based on (i) microwells or U-shaped microstructures, or (ii) emulsion/droplets. Within the first category, the cancer cells are injected into the chip through a microchannel and captured by microwells arrays or U-shaped microstructures allowing their aggregation and tumor spheroid formation. This type of microfluidic chip is suitable for long-term culture, due to the continuum turnover of the culture media injected into the chip through the microchannel. For example, Khot et al. (2020) used a 3D printed master to fabricate cell culturing wells in a PDMS layer sandwiched between two transparent PMMA layers, for direct microscope inspection (Fig. 14 A-F). Using this device and culturing under static conditions, they reported on-chip generation of around 250 μm 3D spheroids from human colorectal HT29 adenocarcinoma cell line. Then they demonstrated that seeding the cells through a port placed directly above the cell culturing wells improves the efficiency of 3D spheroids formation up to 100%, with respect to 68% observed in the case of flow-driven cell seeding. Following the culturing process, the HT29 spheroids were treated and analyzed on chip, through the perfusion of anti-cancer 5-Fluorouracil and the use of fluorescence microscopy for subsequent cell viability imaging confirmed by a Lactate dehydrogenase assay on the supernatant. In addition, in this work, two different methods were proposed for administering cytotoxic treatment in the microfluidic devices, specifically limited-perfusion and continuous flow. In the first setup, allowing single endpoint experiments, single 3D spheroids were treated with 5-Fluorouracil under fluid flow (25 min at 20 μL/min) and then incubated under static conditions (for 24 h). In the second setup, spheroids

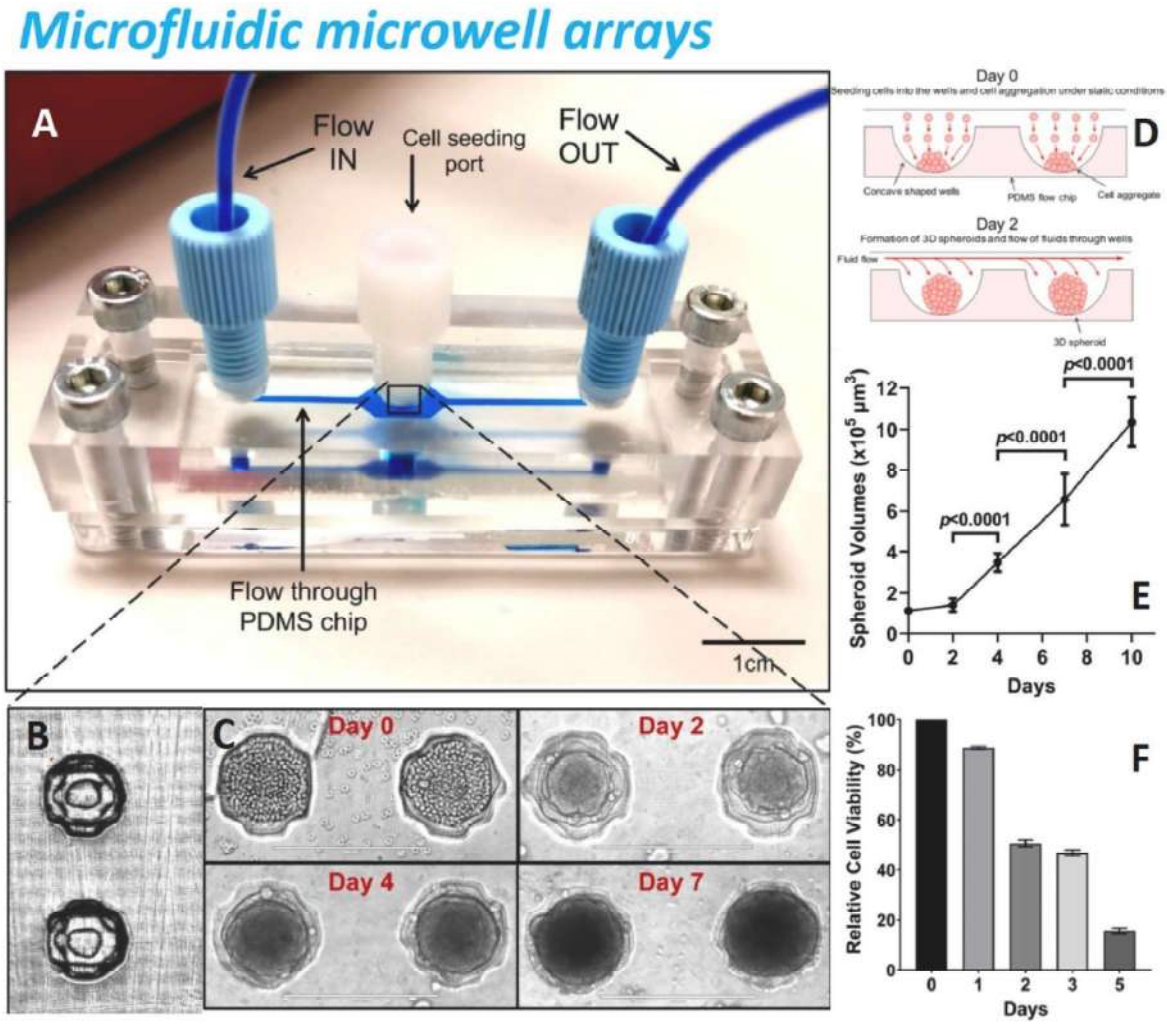

Fig. 14. **(A)** The PDMS 3D cell culturing microfluidic device developed by M. I. Khot et al., embedded between two PMMA layers and using standard UNF 1/4–28 flangeless fluidic fittings. Scale bar = 1 cm. **(B)** Optical microscopic image of the 3D cell culturing wells in the center of PDMS chip. **(C)** Progressive growth of 3D HT29 spheroids in images taken at days 0, 2, 4 and 7. Scale bar = 400 μm. **(D)** Scheme of the designed platform with concave shaped wells to favor cell aggregation at day 0. Then cell aggregates were cultured under static conditions to form 3D spheroids in the following two days and finally fluid flow was applied. **(E)** Progressive growth of HT29 spheroids cultured under static conditions for 10 days in the microfluidic devices. **(F)** The spheroids were treated with 5-FU (200 μM) through continuous perfusion at 20 μL/min for 5 days, and to monitor their chemosensitivity the supernatant was collected at the different time-points to perform a Lactate dehydrogenase (LDH) assay as reported in the histogram. Adapted from Ref. (Khot et al., 2020).

on multiple devices were treated in parallel under continuous perfusion (up to 5 days at 20 μL/min) using a multichannel pump to better mimic systemic circulation in the body. Similar microfluidic chamber arrays were employed for on chip high throughput screening in other sectors/assays, such as screening of transient receptor potential channel modulators (Ai et al., 2020a), screening of species differences in metabolism (Ai et al., 2020b), screening of aggregation models (Mondal et al., 2016), whole-organism behavior-based chemical screening (Chung et al., 2011) and single-embryo screening (Popova et al., 2018).

When the target is high-throughput screening, the use of gradient generators can be very effective. In this respect, Y. Fan et al. (2016) developed a 3D brain cancer chip by using photo-polymerizable poly (ethylene) glycol diacrylate (PEGDA) hydrogel for high-throughput drug screening and prolonged drug release. The relevance of their device lies in the easy fabrication of the microfluidic device by simply a few seconds of photolithography without replica molding and plasma bonding which are instead required in the case of common PDMS microfluidic devices. 3D spheroid formation of glioblastoma multiforme cells (GBM, U87) was achieved into the microwell arrays and the authors investigated a combinatorial treatment with Pitavastatin and Irinotecan exploiting the integration of gradient generators on the chip (Fig. 15A–D).

Tumors, however, are complex tissues typically made of multiple cell types (e.g. cancer and stromal cells). Therefore, heterogeneous spheroids should be generated to explore mutual cell-cell interactions in both spheroids formation and anti-cancer drug screening response. In this respect, Yang et al. (2019) reported the generation of heterospheroids consisting of MCF-7 (breast cancer) and L929 (fibroblast) cells, cultured for a long time in a microfluidic system and treated with Doxorubicin and Paclitaxel. Their device layout consisted of two (microwell and microfluidic) modules. Specifically, the microwell arrays were realized in PEGDA hydrogel, while the microfluidic module was realized in PDMS. Their drug screening study showed that heterospheroids of cancer and fibroblasts cells are characterized by a higher drug-resistance than homospheroids and combinatorial drugs are more effective than single drugs. In another study, Mazzocchi et al. (2018) demonstrated the generation of 3D spheroids in a microfluidic device from cells derived by two mesothelioma biopsies to provide patient-specific models. In general, the microwells arrays approach is suitable for studies on a wider range of drugs, drug combinations and doses, and could represent a powerful tool to adjust patient-specific cancer treatments.

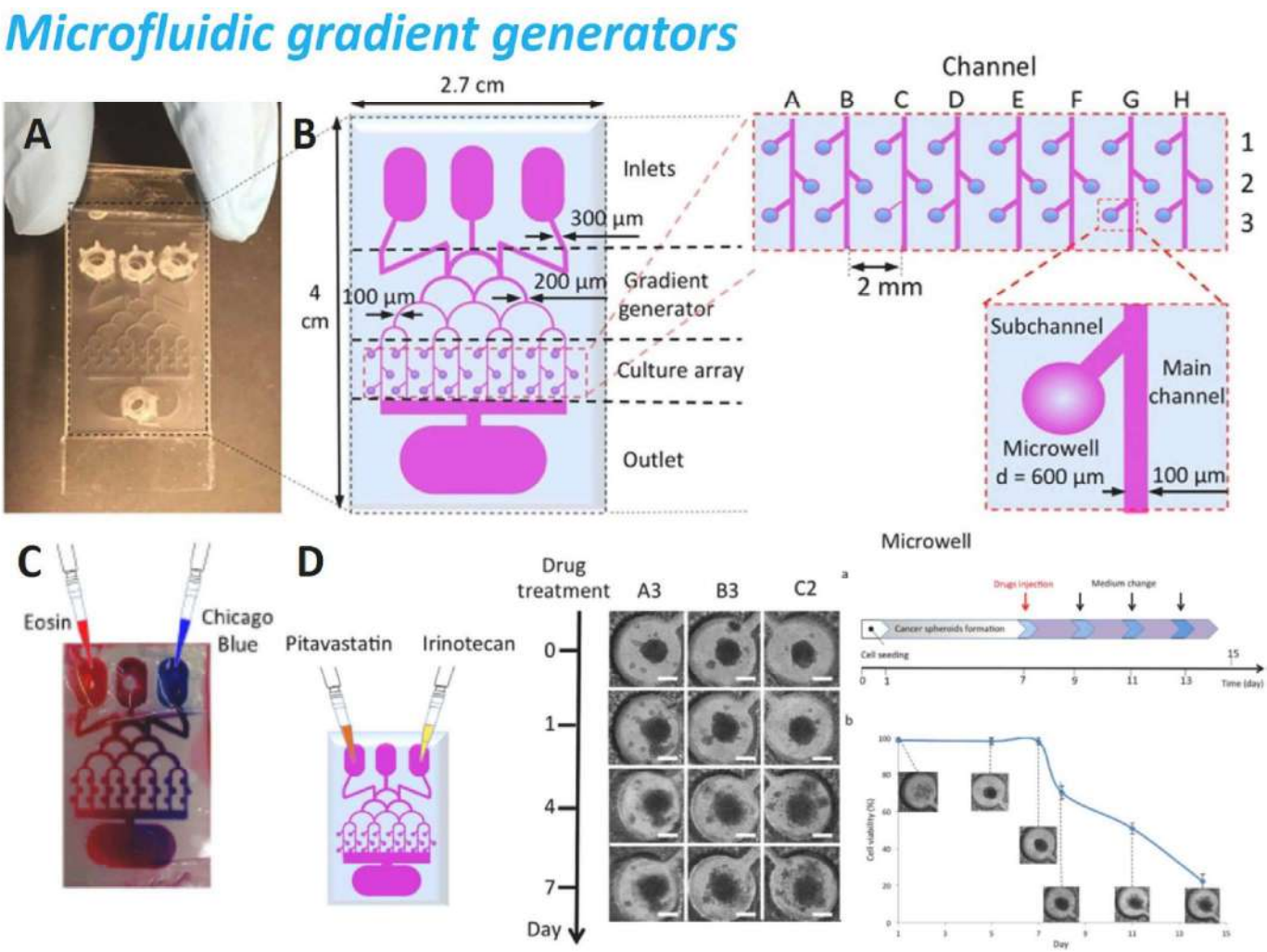

Fig. 15. (A–C) Gradient generator microfluidic chip designed by Fan et al. (Fan et al., 2016) and including individual culture chambers for brain cancer high-throughput combinatorial drug screening, performed with Pitavastatin and Irinotecan on cancer spheroids. **(D)** Time-lapse images and cell viability of U87 cancer spheroids upon continuous drug release. Scale bar, 200 µm. Adapted from Ref. (Fan et al., 2016)

Very promising for cancer research and drug development is the U-shaped microstructures technology reported by W. Liu et al. (2019b), who proposed a microfluidic strategy for large-scale and high-throughput in vitro anti-cancer investigation. An extraordinary large number of heterotypic 3D tumors (total of 672 tumors) with tissue-biomimetic phenotypes were produced in a single microfluidic device. Moreover, on-chip optical and fluorescent imaging were employed to analyze various 3D tumors characteristics such as growth dynamics, viability and apoptosis during cultivation and drug administration. These characteristics are advantageous for standardizing carcinogenesis, tumor progression and drug development studies by means of biomimetic organ-on-chip systems.

Within the second category, droplets microfluidics is exploited. Usually, droplets are generated in a flow-focusing microfluidic device with two incompatible solutions injected in a microfluidic T-junction. At the cross junction, when the solution containing cells in aqueous medium meets the other solution, usually oil, emulsion droplets are spontaneously formed with cells trapped inside, due to their different interfacial properties. Then the droplets can be incubated to favor cells aggregation and tumor spheroid formation. With respect to microwells and U-shaped microstructures, the key advantage with droplets is the large number of microenvironments generated (tens of droplets per second) where cells can be encapsulated with high control on their number and in a rapid and efficient manner. In this frame, Lee et al. (2020) reported a T-junction microfluidic system for large scale generation of cancer-cells embedded in micro-droplets with high generation frequencies (70 Hz) and a generation yield of about 20% higher than previously reported (Kwak et al., 2018). Notably, they demonstrated the fabrication of brain tumor spheroids with diameter tunable between 100 and 130 µm by varying cell concentrations and as proof-of-concept they evaluated photothermal therapy and drug screening responses on brain tumor spheroids.

To resemble the real tumor complexity and microenvironment, cell-laden hydrogel droplets were generated and investigated. In particular, Sabhachandani P. et al. (Sabhachandani et al., 2016) described the generation of cell-laden alginate droplets in a microfluidic device which combines a T-junction for droplet formation and a docking array which can house 1000 droplets for gelation and spheroid formation and on chip drug screening (Fig. 16 A-D). They demonstrated the generation of three spheroids models, drug resistant or drug sensitive breast cancer spheroids (MCF7) and co-culture spheroids consisting of drug sensitive breast cancer cells and fibroblast cells (HS-5). With this technology, they carried out on-chip cytotoxicity experiments using doxorubicin and paclitaxel chemotherapeutic drugs. Jang M. et al. (Jang et al., 2017) used a flow focusing microfluidic platform to generate two different types of 3D in vitro gastric cancer models by using the AGS (intestinal type) and Hs746T (diffuse type) cell lines encapsulated in Type 1 collagen beads (as ECM hydrogel). During droplets formation, the syringe filled with

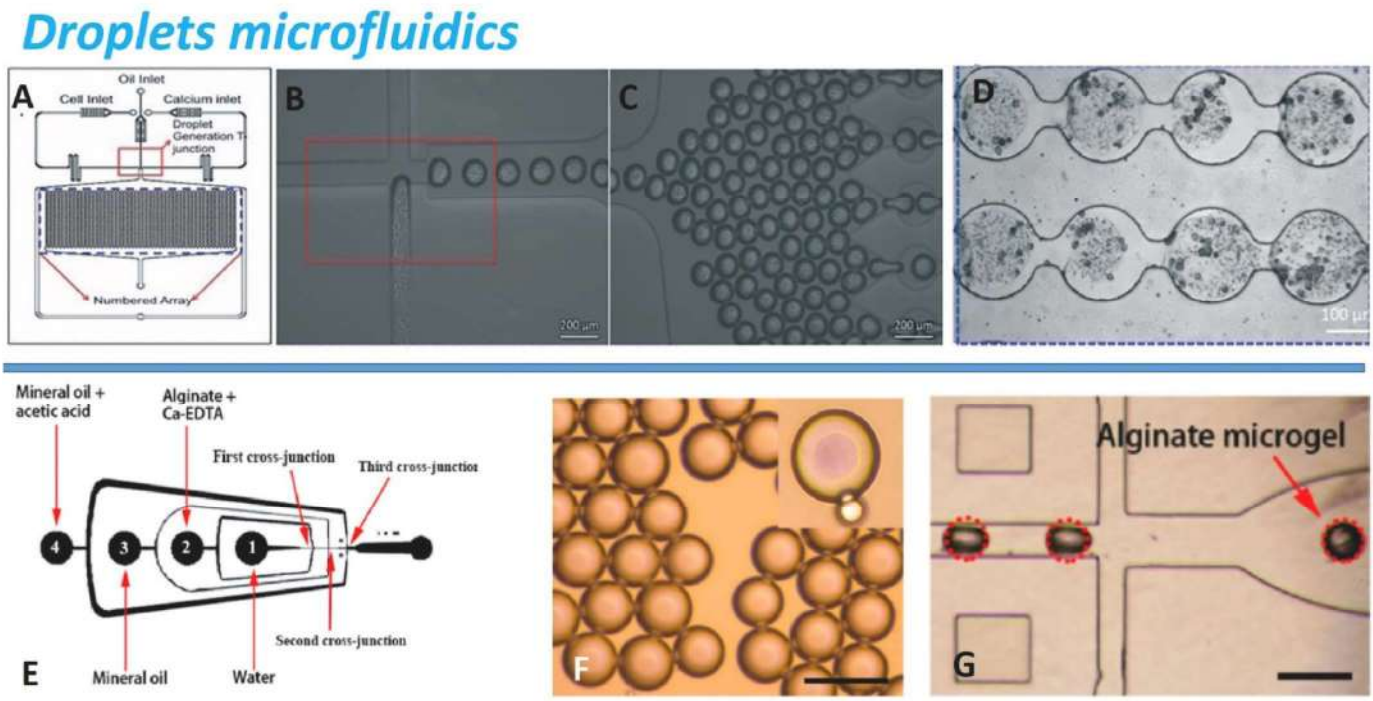

Fig. 16. **(A)** Layout of the microfluidic device for spheroid generation and docking array reported by Sabhachandani et al. (Sabhachandani et al., 2016). **(B)** T-junction for cell-laden alginate droplet formation. Scale bar: 200 μm. **(C)** Droplets entering the docking array after generation but before gelation. Scale bar: 200 μm. **(D)** Docking array with gelled cell-laden alginate spheroids. Scale bar: 100 μm. Adapted from Ref. (Sabhachandani et al., 2016). **(E)** Schematic of the flow-focusing device reported by Sun et al. (Sun et al., 2018) for producing core−shell alginate particles for encapsulating different cells in their core and the shell region. **(F)** Monodispersed core−shell alginate particles collected in mineral oil. **(G)** Cross-linking of alginate and microgel formation due to the injection of mineral oil containing acetic acid which triggers the release of Ca^{2+} from Ca-EDTA. Scale bars are 200 μm. Adapted from Ref. (Sun et al., 2018)

collagen solution was kept at low temperature by means of an ice bag, since collagen gels at 37 °C. Drug screening assays were then performed with 5-fluorouracil on the cultured microtumors. Another employed extracellular matrix component was matrigel, which is characterized by similar temperature dependent properties as collagen type I. Wu et al. (2020) demonstrated the generation in matrigel droplets of tumor spheroids derived from patients' breast tumor tissues. A combined approach was proposed by Karamikamkar et al. (2018), who produced breast cancer spheroids with alginate and collagen as ECM components, since the alginate helps to maintain the spherical shape of beads due to its fast gelling properties with respect to collagen I which gels more slowly and is temperature-sensitive. To reproduce the tumor complexity, Sun et al. (2018) developed a microfluidic layout based on the flow-focusing principle for the preparation of core−shell alginate particles, which permitted the encapsulation of stromal fibroblast cells in the shell and tumor cells in the core (Fig. 16 E-G).

To summarize, today several microfluidic tools are at the disposal of researchers for the implementation of OOC platform and to facilitate high throughput investigations. They include vascularization techniques and perfusable channels, microwell arrays, gradient generators and droplet microfluidics. Beyond them, it is worth mentioning also the availability of microfluidic separation tools to isolate specific cell types or molecular analyte for their further analysis or on chip culture (Nagrath et al., 2007; Chen et al., 2014; Wu et al., 2017; Contreras-Naranjo et al., 2017). Furthermore, microfluidic tools can be employed also for the production of drug nanoformulations and injectable liposomes with therapeutic applications (Zizzari et al., 2017; Shah et al., 2008; Shum et al., 2008). Although their discussion is not covered by this review, the interested researchers can find detailed reviews in literature for further readings.

4.2. Sensor integration for real-time analysis

Organs-on-chips provide effective microphysiological systems for biomedical studies and drug development. However, to take full advantage of their capabilities and accelerate research, they should be combined with efficient analytical methods. In this respect, we can distinguish among (1) endpoint analysis, (2) effluent collection and supernatant based assays, (3) in situ microscopy and imaging characterization and (4) real time analysis with integrated on-chip sensors. Concerning the first two categories, the small volumes in OOC platforms pose some challenges in the use of traditional methodologies such as a possible reduction in the low signal-to-noise ratios (Bennet et al., 2021). Within the third category, fluorescence and confocal microscopy provide powerful tools for investigating cellular arrangement, interactions and processes using appropriate fluorescent staining or tracers (as shown in the previous sections) but additional analytical assays may be required for further insight. In this respect, a recent trend consists in the on chip integration of in-line miniaturized sensors to replace off chip assays on manually extracted samples. This approach offers great opportunities for enabling continuous and automated data collection and in-situ monitoring of functional indicators and biological responses (Marrero et al., 2021a; Young et al., 2019). It also facilitates real-time decision making. The range of monitorable parameters include barrier integrity, oxygen concentration and inflammation response (e.g., cytokines production) as well as electrical and mechanical signals (Li and Tian, 2018b; Soucy et al., 2019). As a consequence, it is worth spending some words to present the most relevant sensing technologies.

Miniaturized (bio)sensors are widely employed in diagnostics and automated lab on chip platforms, exploiting their high selectivity and sensitivity and integration in portable measurements systems (Arndt et al., 2004; Nguyen et al., 2015; Haes et al., 2004; Baselt et al., 1998; Rizzato et al., 2020). In this respect, electrochemical/impedance

read-out is particularly attractive for miniaturization. Electrochemical sensors in OOC models permit to monitor microenvironment conditions (such as pH and temperature) and analyze metabolic parameters (respiration rate, lactate levels and glucose consumption). Enzyme, protein, aptamers and antibodies can be immobilized on the sensor surface as recognition elements to detect specific markers. For example, oxygenation is an important physiological parameter that impacts on cell metabolism and functionality of a tissue (Atkuri et al., 2007). In the gut, intestinal cells are subjected to different oxygen concentrations: low in the lumen center and high in the intestinal mucosa. Changes in oxygen distribution can be a symptom of bacterial infection and/or gut inflammation (Zeitouni et al., 2016). Amperometry with miniaturized electrodes permits to monitor dissolved oxygen levels by measuring the current produced via oxygen reduction reactions. For this purpose,

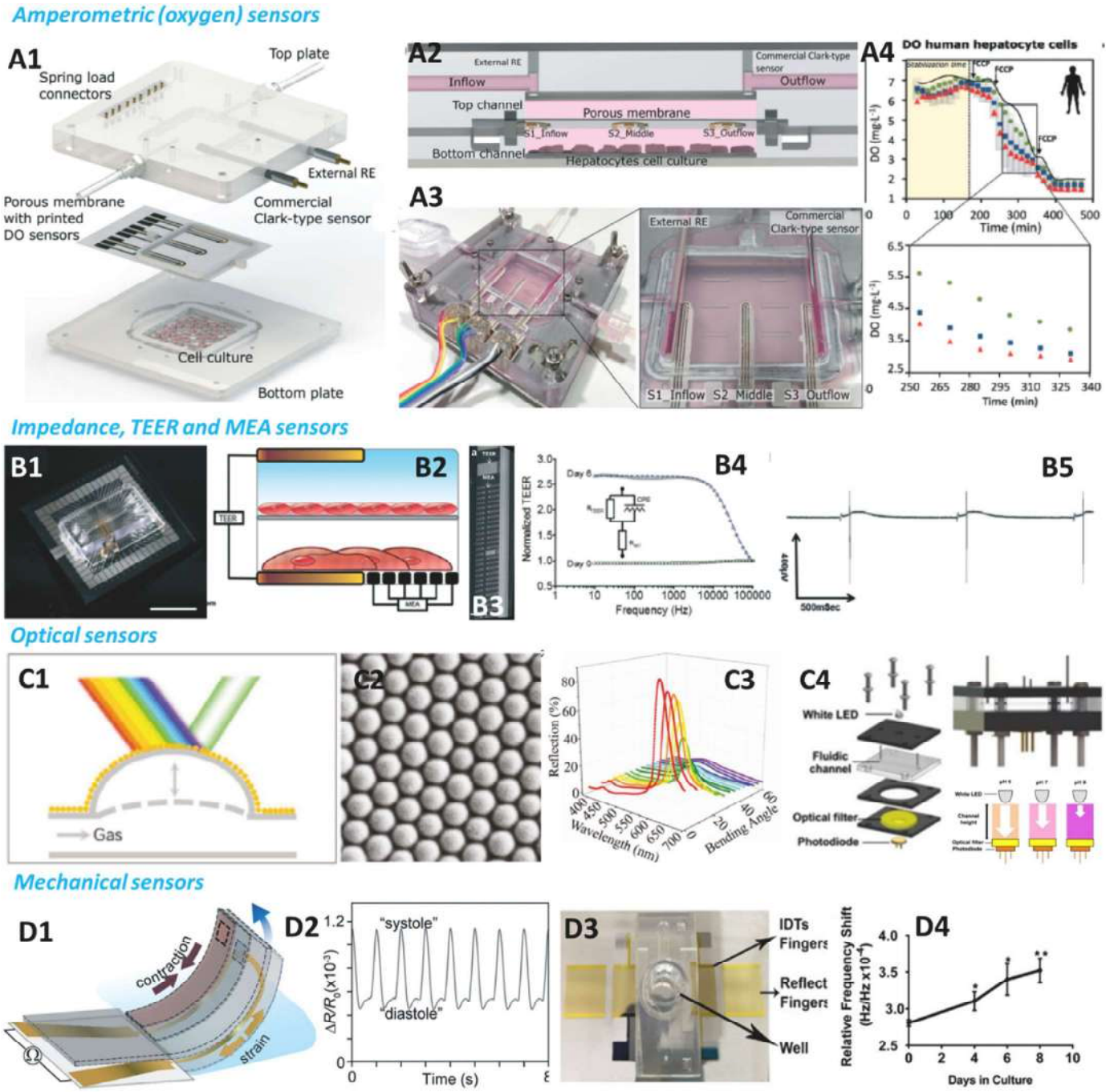

Fig. 17. ***(A1-A4)*** *Schematic of the OOC system with the three printed electrochemical sensors along the microfluidic channel and sensor characterization data without primary cells, with primary rat hepatocytes cell culture, and with primary human hepatocytes* (Moya et al., 2018). ***(B1)*** *Transepithelial Electrical Resistance- Multi-Electrode Array chip.* ***(B2)*** *Schematic of experimental setup with endothelial layer grown on the top of membrane and cardiomyocytes on the top of MEA and among the two sets of TEER electrodes.* ***(B3)*** *Scanning electron microscope (SEM) image of the bottom layer electrodes.* ***(B4)*** *TEER measurements as a function of frequency* ***(B5)*** *MEA trace of single electrode* (Maoz et al., 2017). ***(C1)*** *Schematic diagram of sectional view of the pulmonary alveolus which activity is monitored using photonic nanoparticles* ***(C2–C3)*** (Zhu et al., 1002).***(C4)*** *Optical* pH *sensing in cell culture medium and sensor characterization data.* (Shaegh et al., 2016).***(D1)*** *Cantilever strain-gauge sensor* ***(D2)*** *Micrograph of the sensor and typical response curve.* (Lind et al., 2017b) ***(D3-D4)*** *Surface acoustic wave sensor for detection and quantification of viability and growth of cells* (Wang et al., 2015).